Fabrication of Complex Crystals Using Kinetic Control, Chemical Additives, and Epitaxial Growth

Tzy-Jiun M. Luo,[†] John C. MacDonald,[‡] and G. Tayhas R. Palmore*,[†,§]

Division of Engineering, Brown University, Providence, Rhode Island, 02912, Department of Chemistry and Biochemistry, Worcester Polytechnic Institute, Worcester, Massachusetts 01609, and Division of Biology and Medicine, Brown University, Providence, Rhode Island, 02912

The growth kinetics of crystals of bis(imidazolium 2,6-dicarboxypyridine) M (II) dihydrate, where M = Cu, Ni, Co, Zn, and Mn, were studied in situ using atomic force microscopy. The aspect ratios of specific crystal facets were found to vary systematically with changes in the total concentration of the three components in this crystal system, which can be explained in terms of the growth kinetics at the (100) and (011) faces. Furthermore, inclusion of chemical additives in the growth solutions altered both the habit and faceting of these crystals. Crystallographic analysis of the molecular packing revealed a mechanism by which changes in the habit and faceting occur in the presence of chemical additives. This mechanism was exploited to facet selectively the (001) face for epitaxial studies between crystals containing different metal (II) ions. Epitaxial deposition of crystalline layers containing one metal (II) ion onto the (001) face of a crystal substrate containing a different metal (II) ion was found to be more difficult to achieve when compared to that for the (100) face. To overcome the difficulty of epitaxial growth on the (001) face of these crystals, crystalline gradients were employed, the results of which are demonstrated by the growth of complex crystals with distinct domains of crystal habit and molecular composition.

Introduction

We are interested in using molecular self-assembly to fabricate structures composed of crystalline materials with complex shape and composition. Novel approaches[1,2] to fabricating bulk crystals, patterned crystals, and arrays of crystalline islands and fibers are sought because the morphology, composition, and arrangement of these materials are important in optical, electrooptic, photorefractive, and magnetic applications.[3–9] The advantage of self-assembly over photolithography lies in its bottom-up approach to the fabrication of structures. Molecules spontaneously assemble into crystals that range in size from nanometers to meters, and thus provide a means for fabricating structures far smaller than photolithography can deliver (i.e., 100 nm).[10] The suc-

cessful fabrication of complex crystalline structures via self-assembly requires the development of a crystalline system that can be grown from solution in a controlled manner, and that subsequently can be patterned with a crystalline system of different composition.

In previous studies, we have used molecular design and cocrystallization techniques to produce crystals with specific architecture and periodicity.[11,12] In general, the arrangement of molecules within a crystal is determined by the intrinsic energy of packing and usually is not affected by the manner in which the crystal is grown, with the exception of polymorphic crystals.[1,2,13–24] The manner in which the crystal is grown, however, does affect the habit and faceting of a crystal.[25] For example,

* Corresponding author. E-mail: palmore@brown.edu.
† Division of Engineering, Brown University.
‡ Worcester Polytechnic Institute.
§ Division of Biology and Medicine, Brown University.

(1) Bonafede, S. J.; Ward, M. D. *J. Am. Chem. Soc.* **1995,** *117,* 7853.
(2) Mitchell, C. A.; Yu, L.; Ward, M. D. *J. Am. Chem. Soc.* **2001,** *123,* 10830.
(3) Gatteschi, D., Ed. *Magnetic Molecular Materials*; Kluwer Academic Publishers: Lucca, Italy, 1991; p 411.
(4) Ashwell, G. J. *Molecular Electronics*; Wiley: New York, 1992; p 362.
(5) Bosshard, C.; Sutter, K.; Prêtre, P.; Hulliger, J.; Flörsheimer, M.; Kaatz, P.; Günter, P. *Organic Nonlinear Optical Materials*; Gordon and Breach Science Publishers: Switzerland, Postfach, 1995; Vol. 1.
(6) Wright, J. D. *Molecular Crystals*; Cambridge University Press: New York, 1995.
(7) Aakeröy, C. B.; Beatty, A. M. *Cryst. Eng.* **1998,** *1,* 39.
(8) Bailey, R. D.; Hook, L. L.; Powers, A. K.; Hanks, T. W.; Pennington, W. T. *Cryst. Eng.* **1998,** 1.
(9) Fraxedas, J. *Adv. Mater.* **2002,** *14,* 1603.
(10) Whitesides, G. M.; Mathias, J. P.; Seto, C. T. *Science* **1991,** *254,* 1312.

(11) Palmore, G. T. R.; Luo, T. J. M.; McBride-Wieser, M. T.; Picciotto, E. A.; Reynoso-Paz, C. M. *Chem. Mater.* **1999,** *11,* 3315.
(12) Luo, T.-J.; Palmore, G. T. R. *Cryst. Growth Des.* **2002,** *2,* 337.
(13) Bernstein, J. *Polymorphism in Molecular Crystals*; Oxford University Press Inc.: New York, 2002; Vol. 14.
(14) Desiraju, G. R. *Crystal Engineering: The Design of Organic Solids*; Elsevier: Amsterdam, 1989; Vol. 54.
(15) Desiraju, G.; Gavezzotti, A. *Acta Crystallogr., Sect. B: Struct. Sci.* **1989,** *45,* 473.
(16) Martin, J. D.; Canadell, E.; Becker, J. Y.; Bernstein, J. *Chem. Mater.* **1993,** *5,* 1199.
(17) Carter, P. W.; Ward, M. D. *J. Am. Chem. Soc.* **1993,** *115,* 11521.
(18) Carter, P. W.; Frostman, L. M.; Hillier, A. C.; Ward, M. D. In *Nucleation and Growth of Molecular-Crystals on Molecular Interfaces— Role of Chemical Functionality and Topography*; ACS Symposium Series; American Chemical Society: Washington, DC, 1994; p 186.
(19) Frostman, L. M.; Bader, M. M.; Ward, M. D. *Langmuir* **1994,** *10,* 576.
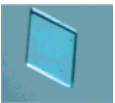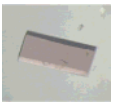(20) Frostman, L. M.; Ward, M. D. *Langmuir* **1997,** *13,* 330.
(21) Rovira, C.; Novoa, J. J. *Chem. Phys. Lett.* **1997,** *279,* 140.
(22) Price, S. L.; Wibley, K. S. *J. Phys. Chem. A* **1997,** *101,* 2198.
(23) Heuzé, K.; Fourmigué, M.; Batail, P.; Canadell, E.; Auban-Senzier, P. *Chem. Eur. J.* **1999,** *5,* 2971.
(24) Yu, L. *J. Am. Chem. Soc.* **2003,** *125,* 6380.

Table 1. Habits and Selected Crystallographic Parameters[39] of Crystals of 1-M Where M = Cu²⁺, Ni²⁺, Co²⁺, Zn²⁺, and Mn²⁺ [a]

typical habit	rhombohedron (e.g., **1-Cu**)		rectangular plates (e.g., **1-Co**)		

metal (II) ion	Cu	Ni	Co	Zn	Mn
largest facet	100	100	001	001	001
a (Å)	10.753(1)	10.596(1)	8.996(2)	8.846(1)	8.931(2)
b (Å)	8.449(1)	8.588(1)	10.302(2)	10.419(1)	10.340(2)
c (Å)	12.840(1)	12.803(1)	12.385(3)	12.315(1)	12.580(3)
β (deg)	103.628(1)	103.764(1)	93.31(3)	92.244(7)	93.00(3)
V (Å³)	1133.6(1)	1131.7(1)	1145.9(4)	1134.2(2)	1160.1(4)
θ^b	77.6°	77.3°	85.1°	85.3°	85.2°

[a] Crystals were nucleated from a solution containing one equiv of metal (II) ion to four equiv each of imidazole and 2,6-dicarboxypyridine dissolved in aqueous DMSO (90% v/v). Crystals containing Co (II) ions sometimes appeared as a rhombic prism, an intermediate morphology between a rhombohedron and a rectangular plate. The value for α and γ in all five crystals is 90°. [b] The angle between the plane of the pyridyl rings and the (001) face of **1-M**.

impurities or additives have been used to change the habit of organic crystals. Additives that have been used include amino acids,[26,27] adipic acid,[28,29] and paraffins,[30] and inorganic crystals such as calcium carbonate,[31–33] calcium oxalate,[34] tin dioxide,[35] barium sulfate,[36,37] and potassium dichromate.[38] These earlier examples illustrate how the shape or design of a material can be controlled with a knowledge of the relationship between the structure of a chemical additive and the surface of the crystal.

This paper describes several methods with which to control the kinetics of growth of crystals of bis(imidazolium 2,6-dicarboxypyridine) M (II) dihydrate, where M = Cu, Ni, Co, Zn, and Mn. These methods were used to select specific crystal facets for subsequent epitaxial deposition and to control the habit of both the substrate crystal and the epitaxial deposit during their growth. Different facets of the substrate crystals were found to promote or inhibit selectively the growth of an epitaxial deposit containing a metal (II) ion different from that of the substrate. The compatibility between specific facets of the substrate crystal and the epitaxial deposit was found to be controllable through the use of crystal gradients. Using a combination of concentration, chemical additives, and crystal gradients, complex multicomponent crystals with specific shapes and compositions were fabricated, representing a first step toward the design of ordered structures with three-dimensional
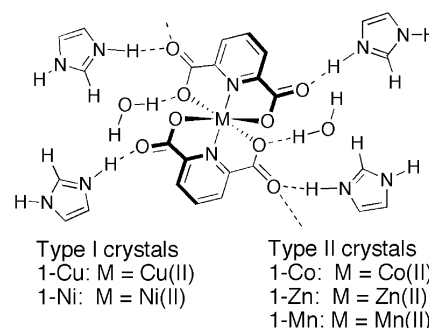
Figure 1. Molecular structure of **1-M**, where M = Cu²⁺, Ni²⁺, Co²⁺, Zn²⁺, and Mn²⁺.

surface features and topologies fabricated via solvent-mediated self-assembly.

Results and Discusson

Structure and Habit of Crystals of Bis(imidazolium 2,6-dicarboxypyridine) metal (II) Dihydrate. We previously reported the crystal structures of bis(imidazolium 2,6-dicarboxypyridine) M (II) dihydrate, where M = Cu, Ni, Co, Zn, and Mn (Figure 1, **1-M**).[39] These solids were designed to test the hypothesis that imidazole would form salts with the metal (II) complex, which consists of two 2,6-dicarboxypyridine ligands coordinated to a metal (II) ion, and that these salts would assemble into robust layers. It was established that the organic components dominate the crystal packing in all five solids, creating a host lattice that accommodates different metal (II) ions without altering the pattern of packing in the crystal.

All five solids crystallize in the same space group ($P2/c$) and have unit cells with dimensions that are summarized in Table 1 and Figure 2.[39] Although the c-dimension and volume occupancy differ at most by 0.53 Å (4.3%) and 28.4 Å³ (2.5%), respectively, there are some notable differences between the five solids. For example, the dimensions of the a and b axes switch on going from **1-Cu** and **1-Ni** to those of **1-Co**, **1-Zn**, and **1-Mn**. This grouping of **1-Cu** and **1-Ni** vs **1-Co**, **1-Zn**, and **1-Mn** also is reflected in the angle β, which is ~10° wider in **1-Cu** and **1-Ni** than that in **1-Co**, **1-Zn**, and **1-Mn**. This same grouping also is evident when the

(25) Cashell, C.; Corcoran, D.; Hodnett, B. K. *Chem. Commun.* **2003**, 374.

(26) Addadi, L.; Berkovitch-Yellin, Z.; Weissbuch, I.; van Mil, J.; Shimon, L. J.; Lahav, M.; Leiserowitz, L. *Angew. Chem., Int. Ed. Engl.* **1985**, *24*, 466.

(27) Weissbuch, I.; Addadi, L.; Lahav, M.; Leiserowitz, L. *Science* **1991**, *253*, 637.

(28) Pfefer, G.; Boistelle, R. *Chem. Eng. Res. Des.* **1996**, *74*, 744.

(29) Williams-Seton, L.; Davey, R. J.; Lieberman, H. F.; Pritchard, R. G. *J. Pharm. Sci.* **2000**, *89*, 346.

(30) Kern, R.; Dassonville, R. *J. Cryst. Growth* **1992**, *1992*, 191.

(31) Davey, R. J. *J. Chem. Soc., Faraday Trans.* **1991**, *87*, 3409.

(32) Raz, S.; Weiner, S.; Addadi, L. *Adv. Mater.* **2000**, *12*, 38.

(33) Aizenberg, J.; Lambert, G.; Weiner, S.; Addadi, L. *J. Am. Chem. Soc.* **2002**, *124*, 32.

(34) Bouropoulos, N.; Weiner, S.; Addadi, L. *Chem. Eur. J.* **2001**, 7, 1881.

(35) Davey, R. J.; Rebello, A. *Cryst. Growth Des.* **2001**, *1*, 187.

(36) Davey, R. J.; Black, S. N.; Bromley, L. A.; Cottier, D.; Dobbs, B.; Route, J. E. *Nature* **1991**, *353*, 549.

(37) Qi, L.; Coffen, H.; Antonietti, M. *Angew. Chem., Intl. Ed.* **2000**, *39*, 604.

(38) Oaki, Y.; Imai, H. *J. Am. Chem. Soc.* **2004**, *126*, 9271.

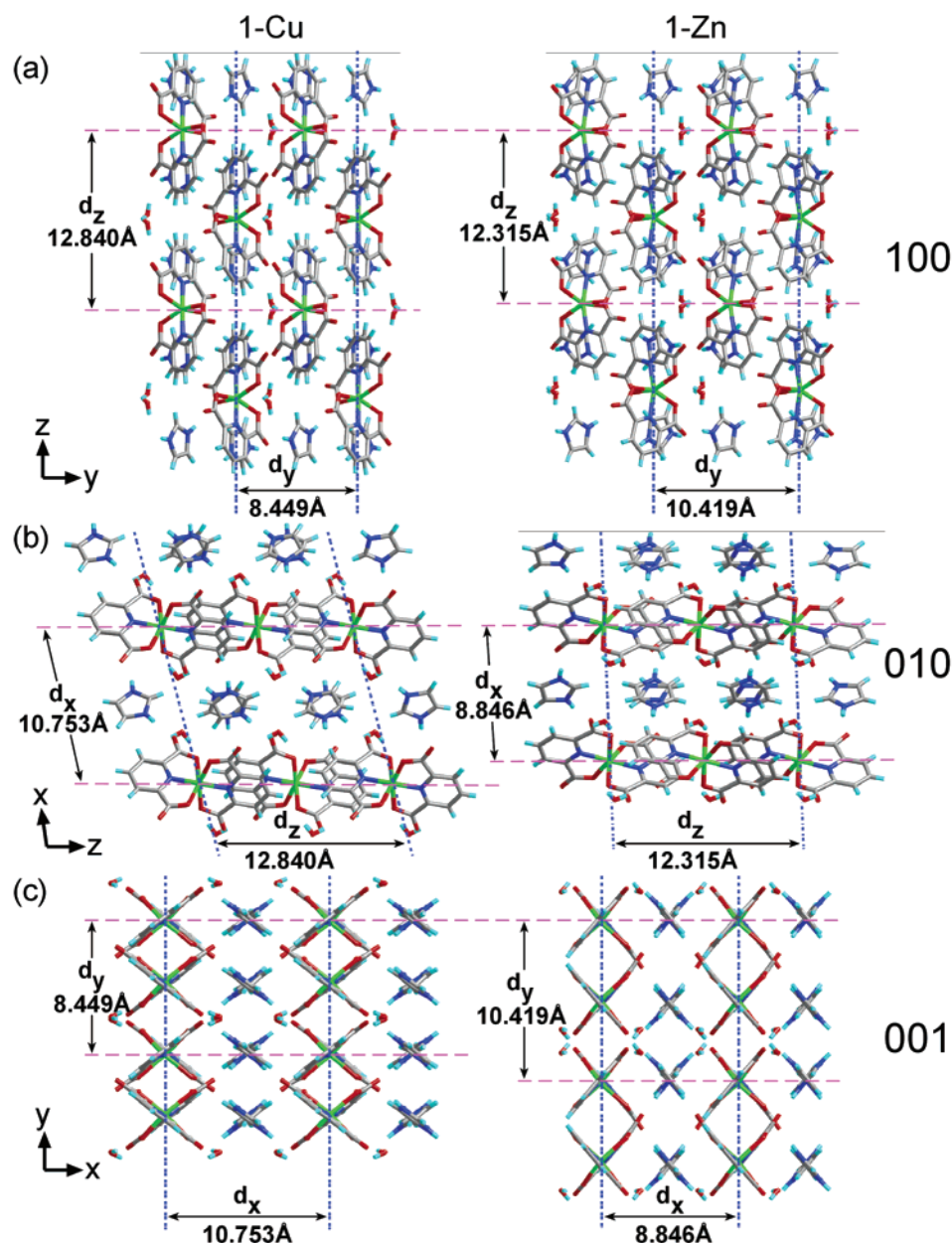(39) MacDonald, J. C.; Dorrestein, P. C. *Trans. ACA* **1998**, *33*, 121.

Figure 2. Packing diagrams oriented to show the (100), (010), and (001) surface of **1-Cu** (representative of **1-Ni**) and **1-Zn** (representative of **1-Co** and **1-Mn**).

geometry of the coordination complex in these crystalline solids is considered, where the N–M–N angle involving the nitrogen atoms on the two pyridyl ligands and the central metal atom changes from nearly linear in **1-Cu** [178.5(7)°] and **1-Ni** [178.1(3)°] to bent in **1-Co** [166.5(9)°], **1-Zn** [166.2(2)°], and **1-Mn** [163.9(4)°].

Despite the variation in the molecular geometry of the coordination complexes, all five solids have similar crystallographic packing that is dominated by hydrogen bonding between imidazolium cations and carboxylate anions. Moreover, the similarity in the crystallographic packing among the five solids permits the growth of composite crystals, where different metal complexes can be segregated in different regions of the crystal (e.g., epitaxial layers grown on the (100) or (011) face of a seed crystal), or mixed crystals, where a mixture of metal (II) ions is present throughout the crystal.[40] An important characteristic of mixed crystals is the ability to vary the physical properties of the crystals such as

color or refractive index by changing the relative ratio of two different metal (II) ions in the growth solution.

Although the crystallographic packing of the five solids is similar, we have observed crystals of these complexes displaying different habits even when grown under identical conditions. For example, crystals grown from solutions containing imidazole, 2,6-dicarboxypyridine, and either Cu (II) or Ni (II) ion, are flattened rhombohedrons with the largest facet being the (100) face. In contrast, solutions containing Co (II), Zn (II), or Mn (II) ions tend to produce crystals of the metal (II) complex that are rectangular plates with the largest facet being the (001) face. For the purpose of the studies describe herein, we have divided the five metal (II) complexes into two

(40) MacDonald, J. C.; Dorrestein, P. C.; Pilley, M. M.; Foote, M. M.; Lundburg, J. L.; Henning, R. W.; Schutlz, A. J.; Manson, J. L. *J. Am. Chem. Soc.* **2000**, *122*, 11692.
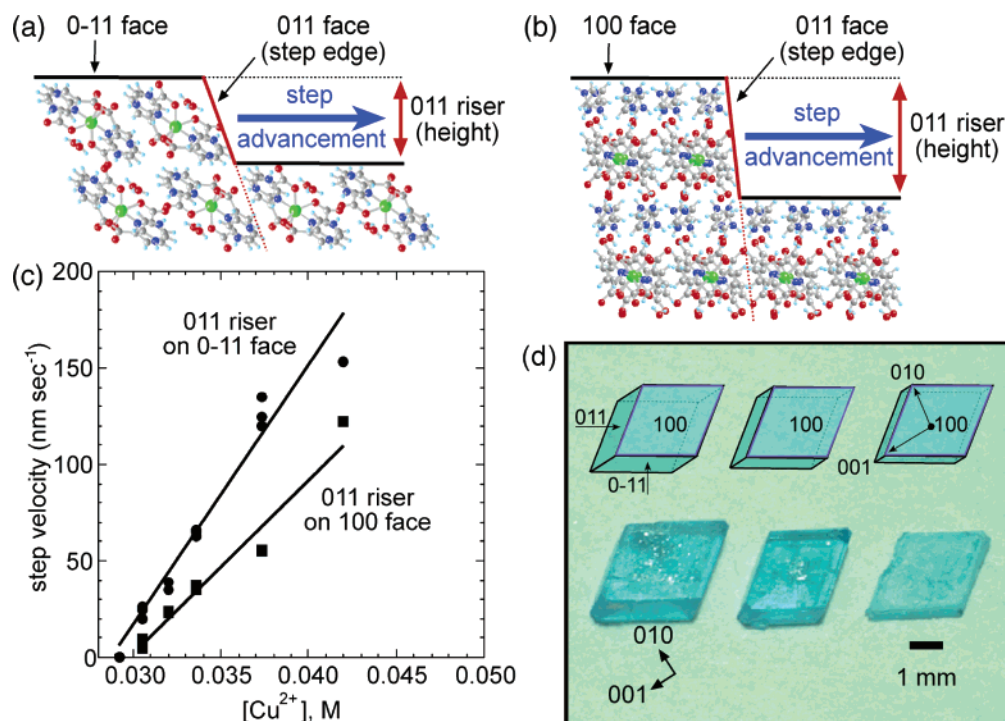
Figure 3. Packing diagram that shows the (011) step riser relative to the (a) (0$\bar{1}$1) face or (b) (100) face. (c) Velocity of the (011) step riser moving across the (0$\bar{1}$1) and (100) faces of a crystal of **1-Cu** plotted as a function of the concentration of Cu (II) ion in the growth solution. All solutions contained a 1:4:4 ratio of Cu (II) ion/imidazole/2,6-dicarboxypyridine. (d) The aspect ratio of a crystal changes when grown from solutions containing an increasing concentration of Cu (II) ion (from left to right, [Cu(II)] = 0.033, 0.042, and 0.056 M). The largest face for all three crystals is the (100) face.

groups according to the habit (rhombohedron or rectangular plates) and dominant facet (100 or 001) of their crystals when grown from a solution containing a 1:4:4 ratio of metal (II) ion/imidazole/2,6-dicarboxypyridine (Table 1).

Effect of Supersaturation on the Habit of Crystals of Bis(imidazolium 2,6-dicarboxypyridine) Metal (II) Dihydrate. Fabrication of complex multicomponent crystals composed of **1-M** necessitates both an ability to control the habit and faceting of the substrate crystal and knowledge as to which crystal can be grown as an epitaxial deposit on a specific facet of that substrate crystal. Supersaturation was examined for its ability to alter the habit, and thus dominant facet, of crystals of **1-Cu** and **1-Ni** to match that of **1-Co**, **1-Zn** and **1-Mn** so that epitaxial growth on the same dominant facet could be compared across the five crystals. One approach to quantifying the effect of supersaturation on crystal habit is to compare the rate at which a step advances across two surfaces of a growing crystal using atomic force microscopy (AFM).[41−47] This technique was used to measure the rate at which the (011)

step-riser advanced across the (100) or (0$\bar{1}$1) facet of a crystal of **1-Cu** growing in solutions containing a 1:4:4 ratio of metal (II) ion/imidazole/2,6-dicarboxypyridine. The (100) and (0$\bar{1}$1) facets were selected because of their prominence in crystals of **1-Cu** and **1-Ni** and their potential sensitivity to changes in supersaturation.

Crystallographic packing diagrams that illustrate the (011) step riser relative to the (0$\bar{1}$1) and (100) faces of **1-Cu** are shown in Figure 3a and b, respectively. The measured height of the (011) step riser was found to be 8 Å when advancing across the (0$\bar{1}$1) face and 10 Å when advancing across the (100) face. Shown in Figure 3c are the velocities at which the (011) step riser moves across the (100) and (0$\bar{1}$1) faces on a crystal of **1-Cu** plotted as a function of the concentration of Cu (II) ion in growth solutions that contain a 1:4:4 ratio of metal (II) ion/ imidazole/2,6-dicarboxypyridine. Although the ratio of the molecular components in the crystals of the five metal (II) complexes is 1:2:2 (metal (II) ion/imidazole/ 2,6-dicarboxypyridine), excess imidazole and 2,6-dicarboxypyridine (e.g., 1:4:4) are included in the growth solution to reduce the overall rate of growth of the crystals. We have shown previously that reducing the overall rate of growth in this manner improves the quality of the crystals and avoids the formation of multiple nuclei.[40] At all supersaturations examined, we found that the velocity of the (011) step riser is faster across the (0$\bar{1}$1) face than it is across the (100) face, thus resulting in a rhombohedron crystal of **1-Cu** with a large (100) face (Figure 3d).

On the basis of the data shown in Figure 3c, the aspect ratio of the (100) and {011} faces can be varied systematically by changing the supersaturation of the growth solution (Figure 3d). For example, faces of nearly

(41) Hillner, P. E.; Gratz, A. J.; Manne, S.; Hansma, P. K. *Geology* **1992**, *20*, 359.

(42) Manne, S.; Cleveland, J. P.; Stucky, G. D.; Hansma, P. K. *J. Cryst. Growth* **1993**, *130*, 333.

(43) Macpherson, J. V.; Unwin, P. R.; Hillier, A. C.; Bard, A. J. *J. Am. Chem. Soc.* **1996**, *118*, 6445.

(44) Palmore, G. T. R.; Luo, T. J.; Martin, T. L.; McBride-Wieser, M. T.; Voong, N. T.; Land, T. A.; DeYoreo, J. J. *Trans. ACA* **1998**, *33*, 45.

(45) Luo, T.-J.; Palmore, G. T. R. *J. Phys. Org. Chem.* **2000**, *13*, 870.

(46) Reviakine, I.; Georgiou, D. K.; Vekilov, P. G. *J. Am. Chem. Soc.* **2003**, *125*, 11684.

(47) Frincu, M. C.; Fleming, S. D.; Rohl, A. L.; Swift, J. A. *J. Am. Chem. Soc.* **2004**, *126*, 7915.
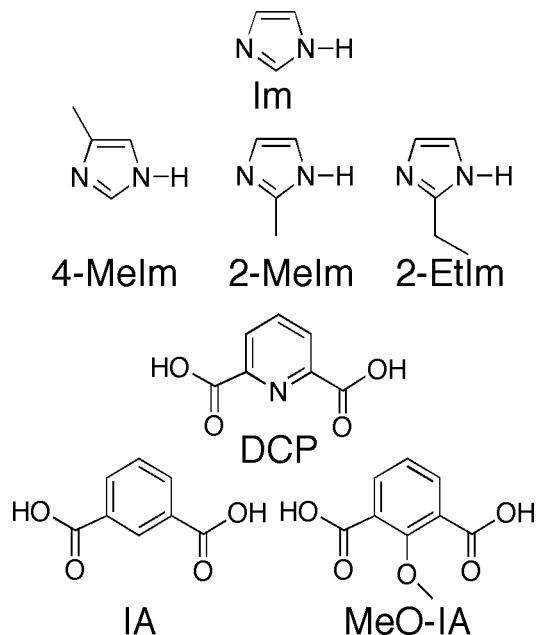
Figure 4. Derivatives of imidazole and 2,6-dicarboxypyridine examined for their ability to change the relative kinetics of crystal growth at different crystal faces and thus the habit of the crystal: imidazole (**Im**); 4-methyl imidazole (**4-MeIm**); 2-methyl imidazole (**2-MeIm**); 2-ethyl imidazole (**2-EtIm**); isophthalic acid (**IA**); and 2-methoxy isophthalic acid (**MeO**−**IA**).

Figure 5. (a) Aspect ratio of y and z in a crystal of the Cu (II) complex plotted as a function of the ratio of **Im** to **4-MeIm** in the growth solution. Growth at the (001) face of **1-Cu** crystals, indicated in red, is inhibited selectively by **4-MeIm**. Similar results were obtained for the Ni (II) complex. (b) Illustration of the relative lengths of y and z in crystals with different habits.

equivalent size develop at low supersaturation because the velocity of the (011) step riser at the (0$\bar{1}$1) face (Figure 3a) is only slightly higher than that at the (100) face (Figure 3b). Conversely, at high supersaturation (e.g., [Cu (II)] ion > 40 mM) the velocity of the (011) step riser at the (0$\bar{1}$1) face is approximately twice as fast as that at the (100) face. Thus, crystals grown at high supersaturation are thin rhombohedrons with the largest facet still being the (100) face. Similar results were obtained for crystals of **1-Ni**.

In contrast, all faces of **1-Co**, **1-Zn**, and **1-Mn** crystals grow significantly slower than those of of **1-Cu** and **1-Ni** crystals when grown under the same conditions (i.e., 1:4:4 mixtures). In addition, the (001) face is the dominant facet in crystals of **1-Co**, **1-Zn**, and **1-Mn**, a facet that does not develop in crystals of **1-Cu** and **1-Ni** grown under the same conditions (cf. Table 1). These two differences, the overall rate of crystallization and the dominant facet, indicate that the excess solute present in the growth solution (i.e., 2-fold excess imidazole and 2,6-dicarboxypyridine) reduces the kinetics of growth at all facets of **1-Co**, **1-Zn**, and **1-Mn** crystals relative to those of **1-Cu** and **1-Ni** crystals and that the kinetics of growth at the (001) facet, in particular, is slower in **1-Co**, **1-Zn**, and **1-Mn** crystals than that of **1-Cu** and **1-Ni**.

Effect of Chemical Additives on the Habit of Crystals of Bis(imidazolium 2,6-dicarboxypyridine) Metal (II) Dihydrate. To determine how chemical additives could be used to alter the habit of **1-M**, crystals of the five complexes were grown in the presence of various amounts of derivatives of imidazole (**4-MeIm**, **2-MeIm**, **2-EtIm**) or isophthalic acid (**IA**, **MeO**−**IA**) (Figure 4). Our objective was to identify chemical additives that could be used to facet selectively the (001) face of **1-Cu** and **1-Ni** crystals so that epitaxial growth
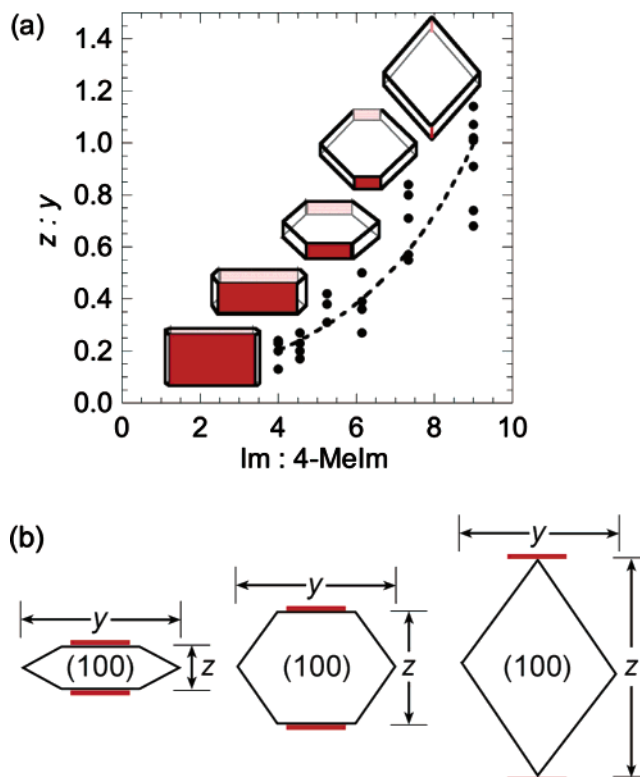
at this surface could be studied and compared to that occurring on the dominant (001) facet of **1-Co**, **1-Zn**, and **1-Mn** crystals. Derivatives of imidazole and isophthalic acids were selected because their molecular shapes are similar to those of imidazole (**Im**) and 2,6-dicarboxypyridine (**DCP**), respectively. Compounds **4-MeIm**, **2-MeIm**, and **2-EtIm** however, will occupy a larger volume than **Im** at the surface of crystals of **1-M** and compounds **IA** and **MeO**−**IA** lack the ability to coordinate metal (II) ions in a tridentate geometry similar to **DCP**.

Depending on the concentration of the chemical additives, all of these compounds changed the habit of **1-Cu** and **1-Ni** crystals to some extent, but **4-MeIm** produced the greatest change. Figure 5a illustrates how the habit of a crystal of **1-Cu** can be varied with changes in the ratio of **Im** to **4-MeIm** in the growth solution. The values of z and y, defined as the length of the crystal as shown in Figure 5b, were measured for all crystals harvested from a growth solution containing different amounts of **4-MeIm**. In the absence of **4-MeIm**, the ratio of z to y for a rhombohedron habit is greater than 1.0. With increasing amounts of **4-MeIm**, the value of z decreases while y remains unchanged.

Without becoming incorporated into the crystalline lattice, **4-MeIm** selectively inhibits growth at the (001) face of **1-Cu** and **1-Ni** crystals. The ratio of z to y can be adjusted to as low as 0.2 when **4-MeIm** is 30% of the total amount of imidazole in the growth solution. Crystals do not grow when the amount of **4-MeIm** exceeds 30% of the total amount of imidazole in the growth solution. Thus, by using the data shown in
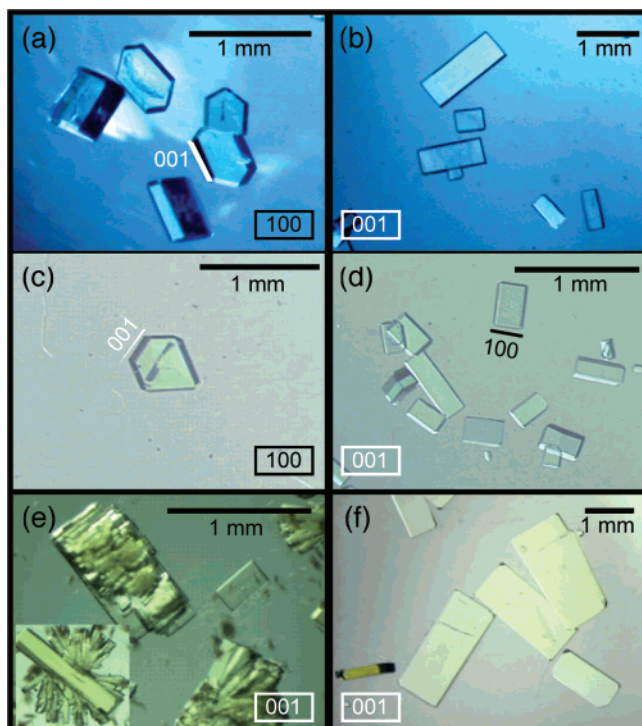
Figure 6. Photos of crystals **1-Cu** (a and b) or **1-Ni** (c and d) nucleated in solutions containing either a 9:1 (a and c) or 8:2 (b and d) ratio of **Im** to **4-MeIm**. Photos of crystals of **1-Mn** (e and f) nucleated in solutions containing either no **4-MeIm** (e) or a 9:1 ratio of **Im** to **4-MeIm** (f). The rectangular box in all photos identifies the crystal face [(100), black; (001), white] projected into the plane of the page.

Figure 7. (a) Crystal of **1-Cu** grown from a solution containing a 1:4:4 ratio of Cu (II) ion/imidazole/2,6-dicarboxypyridine. (b) A growth solution containing **4-MeIm** was seeded with the crystal in (a) and after 1 day of growth the habit of the crystal evolved from a rhombohedron to a rhombic-prism as a result of epitaxial growth. The magnification and orientation of the crystal in (a) and (b) is identical with the original seed crystal from (a) visible within the crystal in (b). (c) A crystal of **1-Cu** grown from a solution containing **4-MeIm**. (d) A solution containing a 1:4:4 ratio of Cu (II) ion/imidazole/2,6-dicarboxypyridine was seeded with the crystal in (c) and after 1 day of growth, the habit of the crystal evolved from a rectangular plate to a half rhombic-prism, an intermediate habit found during the evolution from a rectangular plate to a rhombohedron. The rectangular box in all photos identifies the crystal face projected in the plane of the page.

Figure 5, the habit of **1-Cu** and **1-Ni** crystals can be selected to produce a dominant (001) facet. Similar to crystals of **1-Cu** and **1-Ni**, crystals of **1-Co**, **1-Zn**, and **1-Mn** become thinner (i.e., *z* decreases) when **4-MeIm** is present in the growth solution, however, their habits remain as rectangular plates (cf. Table 1).

To illustrate selective control over the habit of **1-Cu** crystals using **4-MeIm**, shown in Figure 6a are crystals of **1-Cu** nucleated from a solution containing both imidazole and 4-methylimidazole (e.g., **Im/4-MeIm** = 9:1). The resulting crystals are rhombic prisms with the longest axis corresponding to the *b*-axis. Increasing the concentration of **4-MeIm** in the growth solution (e.g., **Im/4-MeIm** = 8:2) results in the formation of fewer nuclei, and because **4-MeIm** inhibits growth at the (001) face, the nuclei develop into thin rectangular plates (Figure 6b). Depending on the amount of **4-MeIm** in the growth solution, **1-Ni** also nucleates into various crystal habits ranging from rhombohedrons to rhombic prisms to rectangular-shaped plates. Figure 6c and d show that the habit of crystals of **1-Ni** can be changed from rhombic prisms to thin rectangular plates using the same protocol used to control the habit of crystals of **1-Cu**. In contrast to what is observed for crystals of **1-Cu** and **1-Ni**, crystals of **1-Co**, **1-Zn**, and **1-Mn** nucleate as rectangular plates in the absence of **4-MeIm**. When **4-MeIm** is present in solution, however, the thickness along the *c*-axis of **1-Co**, **1-Zn**, and **1-Mn** crystals decreases. To illustrate, shown in Figure 6 are crystals of **1-Mn** that were nucleated in the absence (Figure 6e) or presence (Figure 6f) of **4-MeIm** (e.g., 9:1 ratio of **Im** and **4-MeIm**). These results demonstrate that the habits of **1-Cu** and **1-Ni**, in particular, can be
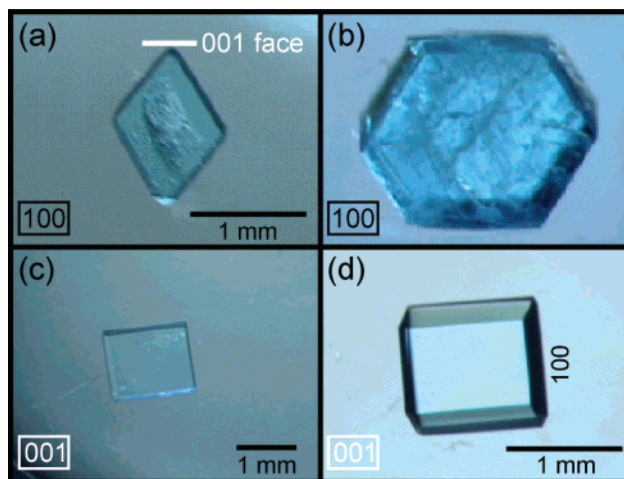
altered selectively by including **4-MeIm** as an additive to the growth solution.

To further illustrate selective control over the habit of **1-Cu** or **1-Ni** crystals using **4-MeIm**, crystals of **1-Cu** or **1-Ni** grown in the absence of **4-MeIm** were used as seed crystals for epitaxial growth in the presence of **4-MeIm**. For example, shown in Figure 7a is a crystal of **1-Cu** grown from a solution containing a 1:4:4 ratio of metal (II) ion/imidazole/2,6-dicarboxypyridine, which produces a rhombohedron habit. When this crystal is placed into, or seeds, a second growth solution where 4-methylimidazole (**4-MeIm**) is substituted for imidazole, the subsequent epitaxial growth exhibits a rhombic-prism habit because **4-MeIm** inhibits the rate of growth at the (001) face. Consequently, the overall habit of the crystal changes from a rhombohedron to a rhombic prism (Figure 7b), and at higher concentrations of **4-MeIm** it changes to rectangular plates.

The inverse experiment gives analogous results. Crystals of **1-Cu** grown from a solution containing a 1:4:4 ratio of metal (II) ion/imidazole/4-methylimidazole/2,6-dicarboxypyridine are rectangular plates with a dominant (001) facet (Figure 7c). When this crystal seeds a second growth solution that does not contain **4-MeIm**, the habit of the epitaxial crystal is rhombohedral-shaped with the (100) face being the slowest growing. Consequently, the overall habit of the crystal evolves from a thin rectangular plate with the (001) face being the slowest growing face (i.e., largest) to a rhombohedron with the (001) face becoming quite small.[48] Shown in Figure 7d is an intermediate crystal

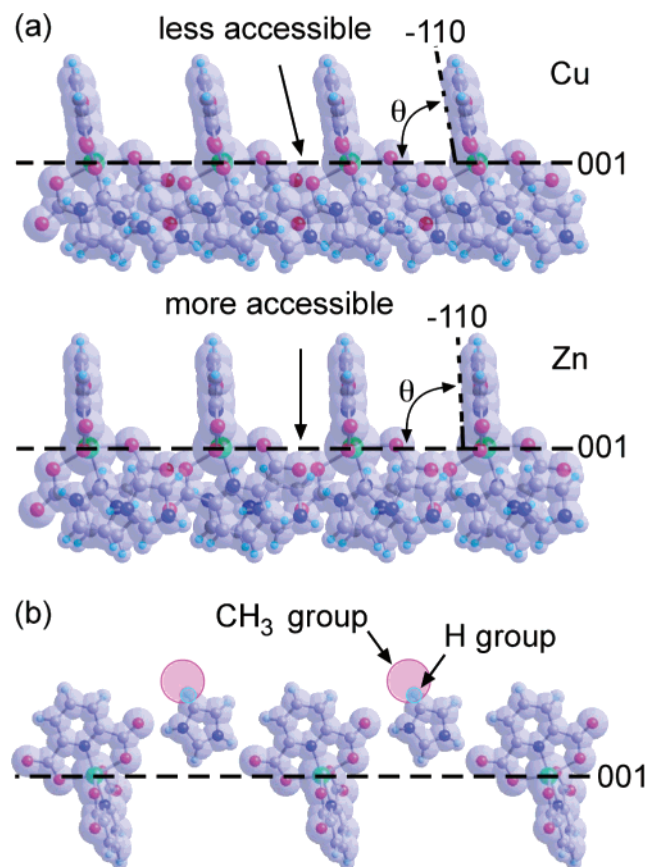(48) Prywer, J. *Cryst. Growth Des.* **2002**, *2*, 281.

Figure 8. (a) Edge-view of (001) face as viewed perpendicular to the (110) face. This perspective illustrates the parallel packing of pyridyl rings and the location of incoming growth units or excess solute molecules (indicated by arrow). (b) Edge-view of (001) face as viewed perpendicular to the ($\bar{1}$10) face. This perspective illustrates the packing of imidazolium cations between the pyridyl rings of adjacent metal (II) complexes. The pink ball on imidazole indicates the location of the methyl group of **4-MeIm** on the (001) surface when **4-MeIm** occupies this site.

habit that develops during the evolution from a thin rectangular plate to a thick rhombic-prism. This intermediate habit (i.e., half of a rhombic-prism) reveals the developing (100) facet and the decreasing size of the (001) facet relative to the (011) and (0$\bar{1}$1) facets.

Mechanism for Changing the Habit of 1-Cu or 1-Ni Crystals with 4-MeIm. The (001) face of **1-Cu** and **1-Ni** crystals does not develop unless **4-MeIm** is included in a growth solution that contains a 1:4:4 ratio of metal (II) ion/imidazole derivative/2,6-dicarboxypy-ridine. Details in the molecular packing at the (001) surface reveal why the (001) face develops in crystals of **1-Co**, **1-Zn**, and **1-Mn** but not in crystals of **1-Cu** and **1-Ni** when grown in the absence of **4-MeIm**, and also why **4-MeIm** inhibits growth at the (001) face more effectively than the other chemical additives studied.

Shown in Figure 8 is an edge-view of the arrangement of the molecular constituents at the (001) surface of the metal (II) complexes viewed perpendicular to either (a) the (110) face or (b) the ($\bar{1}$10) face. The angle (θ), measured between the (001) plane and the plane of the pyridyl rings of the metal (II) complexes, is different for each of the five metal (II) complexes studied although the angle varies by only 0.3° between **1-Cu** and **1-Ni** and by only 0.2° among **1-Co**, **1-Zn**, and **1-Mn** (cf. Table

1). The larger angle associated with **1-Co**, **1-Zn**, and **1-Mn** indicates that the protruding pyridyl rings are nearly orthogonal to the (001) face resulting in a kink site that is more susceptible to being inhabited by excess solute molecules (i.e., 2-fold excess imidazole and 2,6-dicarboxypyridine) than a kink site with a small angle. Occupancy of a kink site by excess solute molecules impedes the addition of a new growth unit (i.e., pyridyl ring of an incoming metal (II) complex) at this site.[49–52] Consequently, the rate of growth at the (001) face is reduced, causing the (001) face to be the dominant facet on crystals of **1-Co**, **1-Zn**, and **1-Mn** grown from a solution containing a 1:4:4: ratio of metal (II) ion/ imidazole/2,6-dicarboxypyridine. In contrast, θ is smaller in **1-Cu** and **1-Ni** than in **1-Co**, **1-Zn**, and **1-Mn**. As a result, the probability of any excess solute molecules other than a growth unit occupying this kink site is lower on crystals of **1-Cu** and **1-Ni** than in crystals of **1-Co**, **1-Zn**, and **1-Mn**. The rate of addition of a new growth unit at this site thus remains high and results in the absence of the (001) facet on **1-Cu** and **1-Ni** grown from a solution containing a 1:4:4: ratio of metal (II) ion/imidazole/2,6-dicarboxypyridine. In fact, the fastest direction of growth occurs along the long axis of the rhombohedral-shaped **1-Cu** and **1-Ni** crystals, which corresponds to the (001) surface.

Figure 8b illustrates how **4-MeIm**, which is similar in molecular structure to **Im**, can inhibit growth on the (001) face by occupying the vacancy between the planes defined by two pyridyl rings. Once **4-MeIm** occupies this kink site, the methyl group of **4-MeIm** protrudes outward from the (001) surface, and thus temporarily prevents the binding of any other molecule at this site.[53] The other derivatives of imidazole (**2-MeIm** and **2-EtIm**) interact with this kink site by directing their methyl groups inward toward the (001) face, an orientation that prevents these molecules from forming strong interac-tions with the (001) face. Consequently, the effect of **2-MeIm** and **2-EtIm** on the kinetics of growth at the (001) face is minimal relative to **4-MeIm**. Nucleation of crystals of **1-Cu** and **1-Ni** in the presence of **IA** and **MeO–IA** confirms that the effect of these additives on the kinetics of growth at the (001) face is minimal (data not shown), which also can be attributed to their weak interaction with this surface.

Epitaxial Growth of Metal (II) Complexes on the (100) Face. All five metal (II) complexes can grow as an epitaxial layer on the (100) surface of a crystal of any of the other metal (II) complexes,[40] indicating that the (100) face of these crystals is able to tolerate the small differences in molecular geometry between the coordination complexes (Figure 9a). This tolerance can be attributed to the fact that the (100) surface for all five crystals consists of alternating layers containing imidazolium cations or bis(2,6-dicarboxypyridine) metal (II) anions. Because the cations and anions segregate into distinct layers, the interface between adjacent

(49) Davey, R. J. *J. Cryst. Growth* **1986**, *76*, 637.
(50) Wireko, F. C.; Shimon, L. J. W.; Frolow, F.; Berkovitch-Yellin, Z.; Lahav, M.; Leiserowitz, L. *J. Phys. Chem.* **1987**, *91*, 472.
(51) Davey, R. J.; Milisavljevic, B.; Bourne, J. R. *J. Phys. Chem.* **1988**, *92*, 2032.
(52) Lahav, M.; Leiserowitz, L. *Chem. Eng. Sci.* **2001**, *56*, 2245.
(53) Weissbuch, I.; Leiserowitz, L.; Lahav, M. "Tailor-Made" Addi-tives and Impurities. In *Crystallization Technology Handbook*, 2nd ed.; Mersmann, A., Ed.; Marcel Dekker: New York, 2001; Vol. 12, p 564.
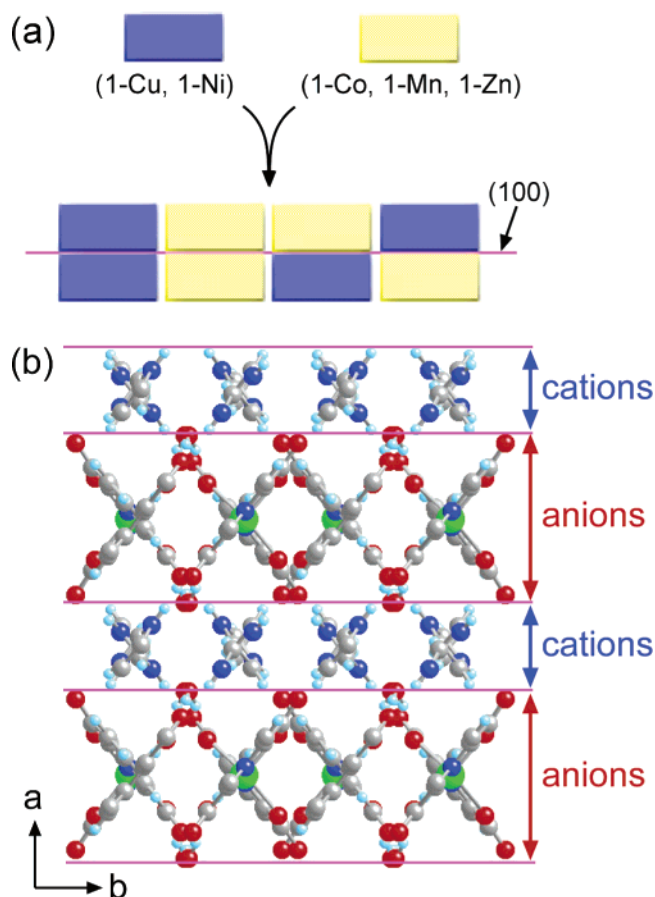
Figure 9. (a) The (100) face of all five crystals of **1-M** can be used as a substrate for the epitaxial growth of any of the other five crystals of **1-M**. (b) Edge-view of the (100) surface (pink lines) of **1-Cu** as viewed perpendicular to the (001) face to reveal the alternating layers of imidazolium cations and bis-(2,6-dicarboxypyridine) Cu (II) anions, a pattern of packing observed in all five metal (II) complexes.

Table 2. Percent Difference in Lengths of Crystallographic Axes[a] in 1-M for Each Combination of Epitaxial Crystal and Substrate Crystal

	Cu	Ni	Co	Zn	Mn
			a-axis		
Cu					
Ni	1.4				
Co	*17.8*	*16.4*			
Zn	*19.5*	*18.0*	1.7		
Mn	*18.5*	*17.1*	0.7	1.0	
			b-axis		
	Cu	Ni	Co	Zn	Mn
Cu					
Ni	1.6				
Co	*19.8*	*18.1*			
Zn	*20.9*	*19.3*	1.1		
Mn	*20.1*	*18.5*	0.4	0.8	
			c-axis		
	Cu	Ni	Co	Zn	Mn
Cu					
Ni	0.3				
Co	*3.6*	*3.3*			
Zn	*4.2*	*3.9*	0.6		
Mn	*2.0*	*1.8*	1.6	2.1	

[a] Values taken from Table 1. Percent difference (e.g., between *a*-axis) = $|a1 - a2|/0.5(a1 + a2)$. Italicized numbers correspond to epitaxial−substrate combinations that involve two crystals from a different group.

layers is smooth (i.e., the anions in one layer do not protrude into the adjacent layers of cations) (Figure 9b).

Consequently, growth at the (100) face of all five crystals involves the repeated assembly of cations followed by anions, a mechanism of assembly that is not available on the (001) face. The implication of this mechanism of assembly is that it permits the lattice spacing of the (100) surface layer of the seed crystal to expand or contract so as to accommodate an incoming epitaxial layer with a different lattice spacing. For example, the percent difference between the *b*-axes and the *c*-axes of the two crystals in each epitaxial−substrate combination that involves two crystals within the same group (e.g., **1-Cu/1-Ni** or **1-Co/1-Zn**), does not exceed 1.6% and 2.1%, respectively (Table 2). Consequently, very little
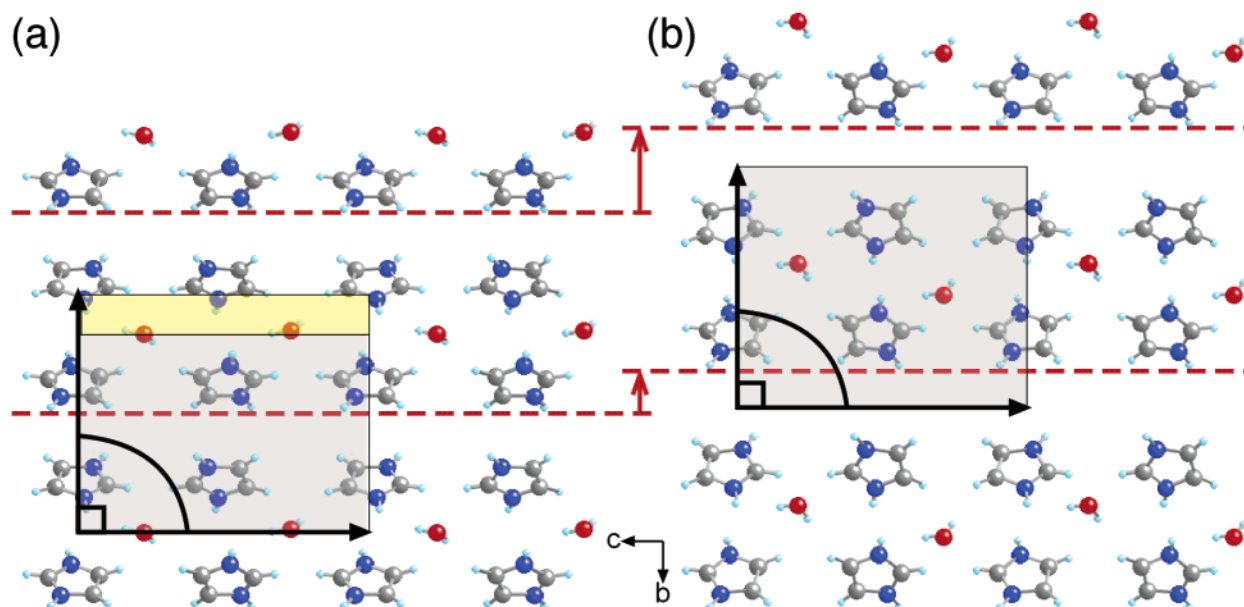

Figure 10. The (100) face of crystals of (a) **1-Cu** and (b) **1-Co**. Only a single layer of imidazolium cations and accompanying molecules of water are shown. The lattice vectors and angle for the (100) face of **1-Co** in (b) has been superimposed onto **1-Cu** in (a) to emphasize that expansion of **1-Cu** primarily along the *b*-axis is required to achieve commensurism with **1-Co**. The transparent gray boxes represent the unit cell for each crystal with their difference represented by the yellow box in (a).
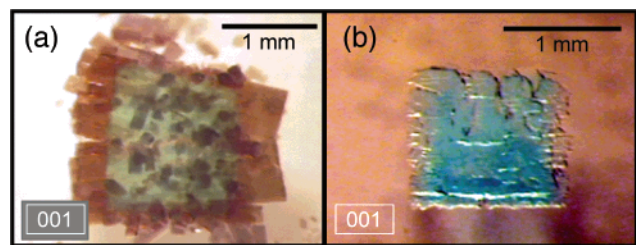
Figure 11. (a) Multiple crystallites of the Co (II) complex nucleate on the (001) face of a crystal of the Cu (II) complex. (b) The seed crystal of the Cu (II) complex dissolved while attempting to grow an epitaxial layer of the Mn (II) complex on the (001) face.

expansion or contraction of the bc-plane is required to achieve a commensurate (100) interface between two crystals from the same group. For epitaxial−substrate combinations that involve two crystals from a different group (e.g., **1-Cu/1-Co** or **1-Ni/1-Zn**), however, the minimum percent difference between the b-axes of the two crystals is 18.1% whereas the maximum percent difference between the c-axes is 4.2% (Table 2). Thus, to achieve a commensurate (100) interface between two crystals from different groups requires expansion or contraction of the lattice, but primarily along only one axis, the b-axis.

To illustrate how this expansion or contraction might occur, shown in Figure 10 are the (100) faces (i.e., bc-plane) of crystals of (a) **1-Cu** (representative of **1-Ni**) and (b) **1-Co** (representative of **1-Zn** and **1-Mn**). Only a single layer of imidazolium cations and accompanying molecules of water are shown. Translation of molecules along the b-axis (indicated by red arrows) in a substrate crystal of **1-Cu** expands its lattice to more closely match that of **1-Co**. Note that despite the long axis in crystals of **1-Cu** and **1-Ni** being defined as the a-axis and the long axis in crystals of **1-Co**, **1-Zn**, and **1-Mn** being defined as the b-axis (cf. Table 1), the orientation of each molecule relative to the coordinate system is the same in all five complexes.

Epitaxial Growth of Metal (II) Complexes on the (001) Face. In contrast to the (100) face, epitaxial growth of **1-Co**, **1-Zn,** and **1-Mn** crystals on the (001) face of **1-Cu** and **1-Ni** crystals and vice versa is more difficult. This difficulty is illustrated by the two examples shown in Figure 11. Seed crystals of **1-Cu**, grown under conditions that facet a large (001) face, were used as substrates for the epitaxial growth of **1-Co** and **1-Mn** crystals. The Co (II) complex nucleates randomly on the (001) face of the underlying seed crystal (Figure 11a) and the Mn (II) complex never grows (Figure 11b) because the seed crystal dissolves.

These results were obtained even though the samples were grown in the same growth solution used to produce epitaxial layers of **1-Co** or **1-Mn** on the (100) face of either **1-Cu** or **1-Ni**. Thus, epitaxial growth on the (001) face is limited to the combinations of crystals that are illustrated in Figure 12a. This limit is attributed to the interlocking nature of the (001) face in which a mixture of cations and anions is presented at the interface between the seed crystal and the epitaxial layer (Figure 12b). The interlocking nature of the (001) face prevents expansion or contraction of the lattice in the ab-plane in the manner described for the bc-plane at the surface of the (100) face. Consequently, epitaxial growth of
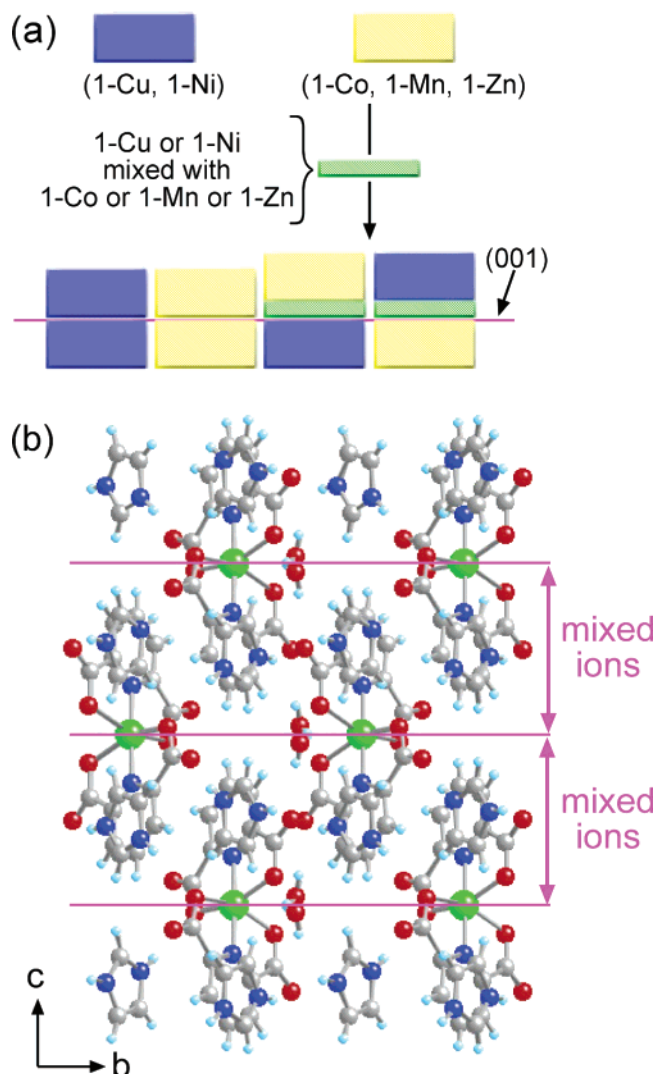

Figure 12. (a) The (001) face of any of the five crystals can be used as a substrate for the epitaxial growth of only crystals of metal (II) complexes with similar values of θ unless an intermediate mixed layer is present. (b) Edge-view of the (001) surface (pink lines) as viewed perpendicular to the (100) surface to reveal the mixed, interlocking layers of imidazolium cations and bis(2,6-dicarboxypyridine) metal (II) anions.

crystalline layers of **1-Co** or **1-Zn** or **1-Mn** at the (001) face of either **1-Cu** or **1-Ni**, and vice versa, requires the incoming metal (II) complex to fit in a kink site defined by the geometry of the metal (II) complex in the underlying seed crystal. Because the angle (θ) between the pyridyl rings and the (001) surface (cf. Figure 8a) differs by 7° between crystals of **1-Cu** and **1-Ni** and crystals of **1-Co**, **1-Zn**, and **1-Mn**, direct epitaxial growth at this surface is incompatible between crystals of **1-Cu** and **1-Ni** and crystals of **1-Co**, **1-Zn**, and **1-Mn**. This incompatibility is revealed further by the percent difference between the relevant lattice parameters of the two crystals in each epitaxial−substrate combination. For epitaxial−substrate combinations that involve two crystals within the same group (e.g., **1-Cu/1-Ni** or **1-Co/1-Zn**), the percent differences between the a-axes and the b-axes of the two crystals are only 1.7% and 1.6%, respectively (Table 2). Consequently, very little expansion or contraction of the bc-plane is required to achieve a commensurate (001) interface between two crystals within the same group. For epitaxial−substrate

Table 3. Sum of the Percent Differences (%d)[a] of the Two Axes Corresponding to the (100) and (001) Face of 1-M for Each Combination of Epitaxial Crystal and Substrate Crystal

(100) %d b-axes + %d c-axes				
	Cu	Ni	Co	Zn	Mn
Cu					
Ni	1.9				
Co	*23.4*	*21.5*			
Zn	*25.1*	*23.2*	1.7		
Mn	*22.2*	*20.3*	1.9	2.9	

(001) %d a-axes + %d b-axes				
	Cu	Ni	Co	Zn	Mn
Cu					
Ni	3.1				
Co	*37.6*	*34.5*			
Zn	*40.3*	*37.3*	2.8		
Mn	*38.6*	*35.6*	1.1	1.7	

[a] Values taken from Table 2. Sum of percent differences for both axes corresponding to a crystal face (e.g., 100 face) = % difference between b-axes + % difference between c-axes. Italicized numbers correspond to epitaxial–substrate combinations that involve two crystals from a different group.

combinations that involve two crystals from a different group (e.g., **1-Cu/1-Co** or **1-Ni/1-Zn**), the minimum percent difference between the two a-axes of the two crystals is 16.4% and the minimum percent difference between the two b-axes is 18.1% (Table 2). Thus, to achieve a commensurate (001) interface between two crystals from a different group requires expansion or contraction of the lattice along *both* the a- and b-axes, a change that is highly improbable due to the interlocking nature of this interface.

Is There a Critical Percent Difference between Relevant Cell Dimensions That is Tolerable for Epitaxial Growth on the (100) Face and (001) Face? A systematic comparison among all five solids reveals that the percent difference in length of the three axes is greatest (italicized numbers in Table 2) when the comparison is between crystals from a different group (i.e., **1-Cu** or **1-Ni** compared with **1-Co**, **1-Zn**, or **1-Mn**). The percent difference in length of the three axes does not exceed 2.1% when the comparison is between crystals from the same group (i.e., **1-Cu** and **1-Ni** or **1-Co**, **1-Zn**, and **1-Mn**). Based on the results shown in Table 2, one might conclude that epitaxial growth of one crystal can occur on the surface of another crystal if the *sum* of the percent differences corresponding to the two axes of a particular face is no greater than 25% (Table 3). This conclusion, however, would be incorrect because it is based solely on a numerical result, which does not take into consideration the molecular structure, molecular geometry, molecular packing, or chemical potential associated with the crystal surface. Nevertheless, the results shown in Tables 2 and 3 reconfirm the experimentally observed grouping of **1-Cu** with **1-Ni** and **1-Co** with **1-Mn** and **1-Zn** based on the previously discussed crystallographic analysis (i.e., the angle β and the N−M−N angle of the coordination complex).

Ward recently reported a lattice-misfit algorithm, EpiCalc, that enables reliable and rapid prediction of the mode of epitaxy (i.e., incommensurism, commensurism, or coincidence) and the optimum azimuthal orientation for a given overlayer−substrate combination, using only the lattice parameters of the overlayer

and substrate as input.[54,55] All possible overlayer−substrate combinations of **1-M** were examined with EpiCalc. Incommensurism was found for all overlayer−substrate combinations containing metal (II) ions from the two different groupings (e.g., **1-Cu** or **1-Ni** on **1-Co** or **1-Zn** or **1-Mn** and vice versa). Coincidence was found when the overlayer−substrate combination contained metal (II) ions within the same group (e.g., **1-Cu** on **1-Ni** or **1-Co** on **1-Zn** and vice versa, but not **1-Cu** or **1-Ni** on **1-Co** or **1-Zn** or **1-Mn** and vice versa). Commensurism was found only when the overlayer−substrate combination consisted of two crystals containing the same metal (II) ion (e.g., **1-Cu** on **1-Cu**). No difference was detected in the EpiCalc data between the (100) and (001) faces in terms of their tolerance to epitaxial growth in the various combinations of overlayer and substrate. Consequently, neither approach (percent difference or lattice-misfit algorithm) explains or predicts the limited combinations of crystals that are observed to yield epitaxial growth on the (001) face of crystals of **1-M**. Instead, an interfacial model based on both molecular structure and molecular packing is more suitable for understanding epitaxial growth between these solids.

Using Gradients to Facilitate Epitaxial Growth on the (001) Face. Although the molecular structures of the anions in all five crystals examined in this study differ slightly, crystals that contain mixtures of two different metal (II) complexes can be prepared by including two different metal (II) ions in the same growth solution.[40] The resulting mixed crystals contain a homogeneous distribution of the different metal (II) complexes in the same relative molar ratio that was present in the growth solution. As a result, an epitaxial layer can be made more compatible with the underlying (001) substrate by introduction of an intermediate layer that contains a mixture of the metal (II) ion of the desired epitaxial layer and the metal (II) ion of the seed crystal (cf., Figure 12a). This method can be used to tune the (001) surface of a **1-Cu** or **1-Ni** crystal for epitaxial growth of a **1-Co** or **1-Zn** or **1-Mn** crystal and vice versa. For example, a percentage of the Co (II) ions in an epitaxial growth solution can be replaced by Cu (II) ions to increase the compatibility of the (001) surface of a **1-Cu** seed crystal toward epitaxial growth of a **1-Co** layer. Similarly, epitaxial growth of **1-Ni** on the (001) face of a **1-Co** seed crystal also can be achieved by adding Co (II) ions to the epitaxial growth solution.

To illustrate the general utility of this method, the (001) face of a seed crystal of **1-Co** can be made compatible toward an epitaxial layer of **1-Cu** by replacing some percentage of the Cu (II) ion in the epitaxial growth solution with a third metal ion, such as Zn (II) ion. In a similar fashion, an epitaxial layer of **1-Ni** can be made more compatible with the (001) face of a seed crystal of **1-Co** by adding Mn (II) ion to the epitaxial growth solution. Similar results are found with seed crystals of **1-Cu** or **1-Ni** and epitaxial layers of **1-Co** or **1-Zn** or **1-Mn**. Alternatively, by including a second metal (II) ion in the initial solution from which a seed crystal is grown, the composition of the (001) surface of the substrate can be modified. One important limitation

(54) Hillier, A. C.; Ward, M. D. *Phys. Rev. B* **1996**, *54*, 14037.
(55) Last, J. A.; Hooks, D. E.; Hillier, A. C.; Ward, M. D. *J. Phys. Chem. B* **1999**, *103*, 6723.
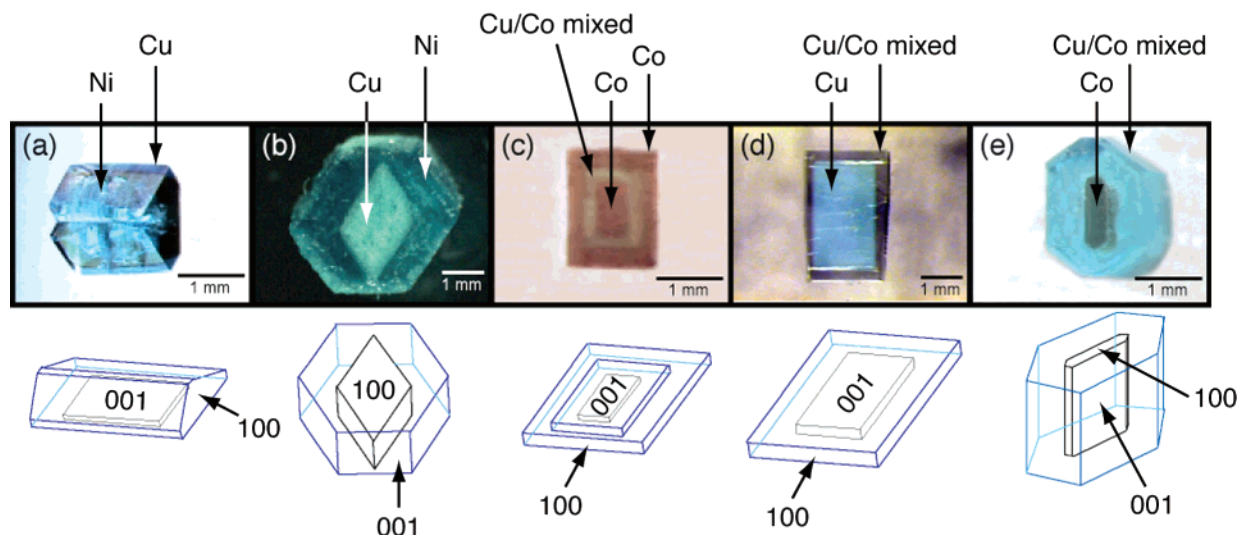
Figure 13. Examples of epitaxial growth on the (001) face of **1-M**. Epitaxial crystal:*seed crystal* are as follows: (a) Cu:*Ni*; (b) Ni:*Cu*; (c) Co:mixed Cu/Co:*Co*; (d) mixed Cu/Co:*Cu*; (e) mixed Co/Cu:*Co*.

is that **1-Cu** or **1-Ni** will not grow uniformly on the (001) face of **1-Co** or **1-Zn** or **1-Mn** in the absence of **4-MeIm**, which is the additive that is required for the (001) face to develop in crystals of **1-Cu** or **1-Ni**, as described earlier.

Growing Complex Crystals. Three factors that affect the growth of crystals of **1-M** have been analyzed: (1) the effect of concentration on the relative velocity of growth at different crystal faces; (2) the effect of chemical additives on the habit and faceting of the crystals; and (3) the compatibility between the dominant facet of a seed crystal and a desired epitaxial layer. Shown in Figure 13 are five examples of complex crystals, which were grown to illustrate that crystals with different shapes and compositions can be fabricated when one or all of these three factors are controlled. Crystals were grown in a microcrystallizer except those shown in Figure 13c and d. All complex crystals were prepared from seed crystals grown from one or a sequence of growth solutions.

To illustrate the use of factors (1) and (2), which affects the aspect ratio of the facets and the dominant facet, a seed crystal of **1-Ni** was grown at higher concentration in the presence of **4-MeIm** to produce a thin plate (i.e., the (100) face is small compared to the (001) face). This seed crystal was used to template the growth of **1-Cu** in the absence of additive, which results in an epitaxial layer whose habit is one-half of a rhombus prism (Figure 13a). To illustrate the use of factor (2), a rhombus prism of **1-Cu** was grown on the surface of a rhombohedral-shaped seed of **1-Ni** (Figure 13b). Crystals of **1-Cu** or **1-Ni** will grow as rhombohedrons in the absence of additives. To generate an outer crystal with a rhombus prism habit, **4-MeIm** was included in the growth solution of **1-Cu** to inhibit growth at the (001) face.

To illustrate the use of factors (2) and (3), a multi-layer, three-domain crystal was prepared (Figure 13c). The seed crystal is a crystal of **1-Co** grown in the presence of **4-MeIm**, which results in rectangular plates. This seed crystal subsequently was encased in a mixed crystal of **1-Cu** and **1-Co**, which then was capped with a surrounding crystal of **1-Co**. Another

illustration of the control of both factors (2) and (3) is to use a crystal of **1-Cu** as a substrate for the growth of a mixed crystal of **1-Co** and **1-Cu** (Figure 13d). Because crystals of **1-Cu** normally grow as a rhombohedral-shaped crystal, the seed crystal was grown in the presence of **4-MeIm** to generate the rectangular-plate morphology (i.e., (001) is the dominant facet). It can be seen from this example that epitaxial growth of the mixed crystal of **1-Co** and **1-Cu** on the seed crystal is more compatible than that of a pure crystal of **1-Co** (cf. Figure 11a). To illustrate control of all three factors, a seed crystal of **1-Co** was used as a substrate for the growth of a mixed crystal of **1-Cu** and **1-Co** (Figure 13e). The seed crystal, grown in the presence of **4-MeIm**, was a thin plate and the mixed crystal, grown at higher concentration in the absence of **4-MeIm**, developed the hexagonal morphology.

Conclusion

Atomic force microscopy was used to study the kinetics of growth of crystals of bis(imidazolium 2,6-dicarboxypyridine) M (II) dihydrate, where M = Cu, Ni, Co, Zn, and Mn. The kinetics of growth at the (001) face is quite different for the five metal (II) complexes despite the similarity in molecular packing in all five of the crystal structures. The differences in growth kinetics manifests as different crystals habits with different dominant facets when grown from solutions of identical concentration that contain a 1:4:4 ratio of metal (II) ion/imidazole/2,6-dicarboxypyridine. On the basis of the different habits obtained, we divided the five metal (II) complexes into two groups. One group consisted of **1-Cu** and **1-Ni**, which grow as rhombohedrons with a dominant (100) facet. The other group consisted of **1-Co**, **1-Zn**, and **1-Mn**, which grow as thin rectangular plates with a dominant (001) facet. Excess solute in the growth solution inhibits the same step edges in all five crystals to a different extent, which results in the appearance of different crystal habits. Several derivatives of imidazole and 2,6-dicarboxypyridine were tested for their ability to alter the habit of the crystals and 4-methylimidazole was found to be the most effective toward crystals of **1-Cu** and **1-Ni**. We demonstrated the use of

4-methylimidazole to change the habit of **1-Cu** and **1-Ni** crystals so that the (001) face was the dominant facet. This change in habit and faceting allowed us to compare epitaxial growth on the (001) face of all five crystals. We found epitaxial growth on the (001) face was more difficult to achieve than on the (100) face but that this difficulty could be overcome by first growing an epitaxial layer consisting of a mixture of **1-Cu** or **1-Ni** with **1-Co**, **1-Zn**, or **1-Mn** (i.e., crystalline gradients). After growth of a crystalline gradient on the (001) face, growth of an epitaxial layer composed of only one metal (II) complex was possible. As a result, crystals of different shape and composition can be grown when factors such as concentration, chemical additives, and gradient epitaxial layers, either alone or in combination, are used selectively. Although the practical utility of these particular solids is yet to be discovered, they illustrate an important prerequisite to building organized structures and topographies via solvent-mediated self-assembly. That prerequisite lies within the modular nature of these solids, where the organic component defines supramolecular structure and the interchangeable metal ion alters the physical properties. Using these materials to build complex topographies will be the subject of future reports.

Experimental Section

Reagents. All regents were purchased from Aldrich and used without further purification. Crystals were obtained by mixing a stock solution containing a 1:4 mixture of metal (II) ion (168 mM) and 2,6-dicarboxypyridine (672 mM) dissolved in aqueous dimethyl sulfoxide (90% v/v) with a stock solution of imidazole (672 mM, either pure or as a mixture of imidazole derivatives) dissolved in aqueous dimethyl sulfoxide (90% v/v).

Crystallization Apparatus. Culture plates with 40 wells each 2 cm in diameter were used for nucleation and epitaxial growth experiments. Stock solutions were mixed to a desired ratio of metal (II) ion, imidazole, and 2,6-dicarboxypyridine and added to each well to a total volume of 1 mL. The wells were covered to avoid contamination (sealing is not required) and subsequently placed in a stable environment. Composite crystals were grown in a microcrystallizer, which consisted of a water-jacketed flask (100 mL) equipped with a rotary stirrer and temperature-controlled water circulator. The general procedure for growing crystals in the microcrystallizer is as follows. First, 40 mL of growth solution was added to the water-jacketed flask and equilibrated to a desired temperature by the water circulator. Next, a seed crystal was mounted to a stirring pad using silicone grease. The stirring pad was attached to the end of a stirring rod connected to a motor that reversed the direction of stirring at a controlled rate and duration. Finally, the mounted crystal was placed in the middle of a water-jacketed flask to initiate new growth.

Nucleation and Growth of Crystals of Bis(imidazolium 2,6-dicarboxypyridine) Metal (II) Dihydrate. In general, equal volumes of each stock solution were mixed at room temperature, resulting in a growth solution composed of a 1:4:4 ratio of metal (II) ion/2,6-dicarboxypyridine/imidazole. Nucleation occurred in highly saturated solutions (i.e., [M(II)] = 0.084 M) with nuclei usually appearing within 24 h. Experiments to measure the kinetics of crystal growth were performed in a saturated solution (66%) containing an equal volume of each stock solution.

Nucleation and Growth of Crystals of Bis(imidazolium 2,6-dicarboxypyridine) Metal (II) Dihydrate in the Presence of Chemical Additives. Stock solutions containing a mixture of imidazole derivatives were prepared by dissolving different ratios of **Im** to **4-MeIm** in aqueous dimethyl sulfoxide (90% v/v) to a combined concentration of 672 mM. These stock solutions subsequently were mixed with an equal volume of the stock solution containing the metal (II) ion and 2,6-dicarboxypyridine.

Velocity of Step Advancement. A PicoSPM by Molecular Imaging was used for all in situ AFM experiments. Single crystals (typically 2×2 mm) of each metal (II) complex were harvested from a growth solution and dried in air at room temperature. Each crystal was indexed and subsequently mounted to the surface of a silanized glass slide using silicone grease. The glass slide with crystal subsequently was placed onto the sample stage of the AFM. A Teflon ring with two ports was seated on top of the glass slide to form a fluid cell, enclosing the mounted crystal. The inlet port of the fluid cell was connected to a vial containing a fresh growth solution and the outlet port was connected to a waste bottle. The total volume of the fluid cell was 600 μL, and the temperature of the solution within the fluid cell was maintained at 25 °C using a peltier temperature controller. For each concentration to be studied, the fluid cell was flushed several times with a growth solution prepared by mixing various amounts of stock solutions described above. During in situ AFM experiments, the growth solution was pumped through the fluid cell at a rate of 10 μL min^{-1}. This rate of flow maintained enough solution within the liquid cell to deliver continuously fresh analyte to the growing crystal. It should be noted, however, that a volume of 600 μL contains enough chemical species to maintain a constant rate of crystal growth for 20 min without the addition of fresh growth solution.

Once contact was made between the AFM tip and the surface of the crystal and during scanning, the set point was adjusted to a maximum value of 0.5 V to limit the amount of force applied to the surface of the crystal. The surface was scanned at a rate of 8−10 line sec^{-1} to generate an image 2 μm × 2 μm in size. The area scanned on the crystal was chosen at random and repeated several times for each injection. The velocity of step advancement at different supersaturations was determined by measuring the acute angle (<90°) between the step-edges in the image and a horizontal line drawn across the image in two consecutive images. This value was substituted into the equation

$$V = \frac{SR}{N} \frac{\cot(\theta_u) + \cot(\theta_d)}{\sqrt{(\cot(\theta_u) - \cot(\theta_d))^2 + 4}} \qquad (1)$$

which gives the velocity of step advancement (V) in units of nm s^{-1} at a particular concentration. In eq 1, S is the scan size (nm), R is scan rate (line s^{-1}), and N is number of lines in each image. During the experiment, the angle between the step-edges in the upward scan (θ_u) and downward scan (θ_d) should be greater than 20° to avoid the intrinsic error of this equation. Kinetic measurements were performed on at least three different crystals to obtain the error range for each data point, which fell within 5%.

CM049121E